

– Supporting Information –

One-step electrodeposition of binder containing Cu nanocube catalyst layers for carbon dioxide reduction

Andrea Serfőző,^a Gábor András Csík,^a Attila Kormányos,^a Ádám Balog,^a Csaba Janáky^a, Balázs Endródi*^a

^a Department of Physical Chemistry and Materials Science, University of Szeged, Rerrich Square 1, Szeged, H-6720 Hungary

*E-mail: endrodib@chem.u-szeged.hu (B. Endródi)

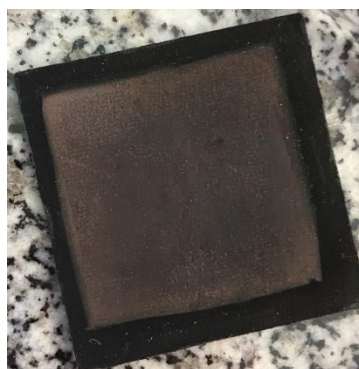


Figure S1. Photograph taken of the Cu NC GDE, formed from a 5 mM CuSO₄/KCl and 15 V/V% isopropanol containing precursor solution, with 500 electrodeposition cycles between (+0.55 V vs. RHE upper vertex potential, +0.22 V vs. RHE with $v = 100 \text{ mV s}^{-1}$ sweep rate.

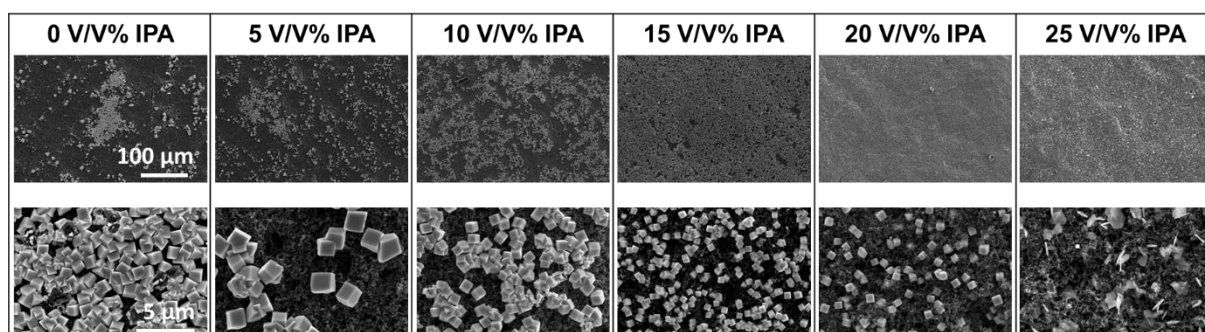


Figure S2. SEM images taken of GDEs prepared by the method presented in Figure 2., but from solutions containing different amount of isopropanol (IPA). The top and bottom row images were captured at 1000x and 25000x magnifications, accordingly.

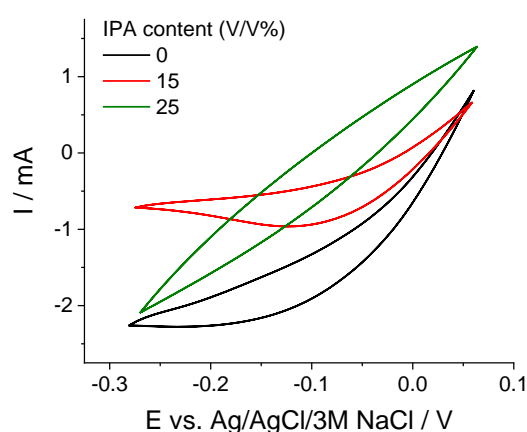


Figure S3. Representative potentiodynamic curves recorded for Cu NC synthesis on Freudenberg H23C6 GDL. The sweep rate was $v = 100 \text{ mV s}^{-1}$, and the measurements were performed at room temperature, in 0, 15 and 25 V/V% isopropanol and 5 mM CuSO₄/KCl containing aqueous solutions. In all cases the 500th cycle is shown for comparison.

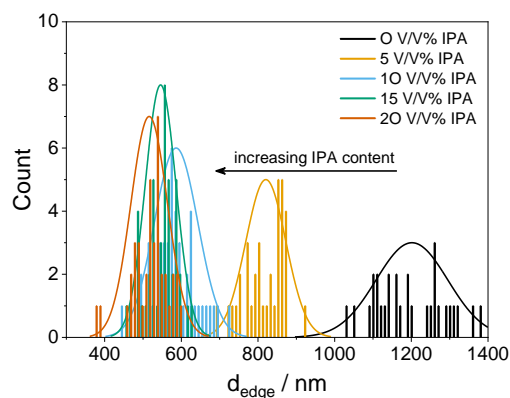


Figure S4 Size distribution of Cu nanocubes formed by electrodeposition from 5 mM CuSO₄/KCl containing solutions with water:IPA solvent mixtures of different composition.

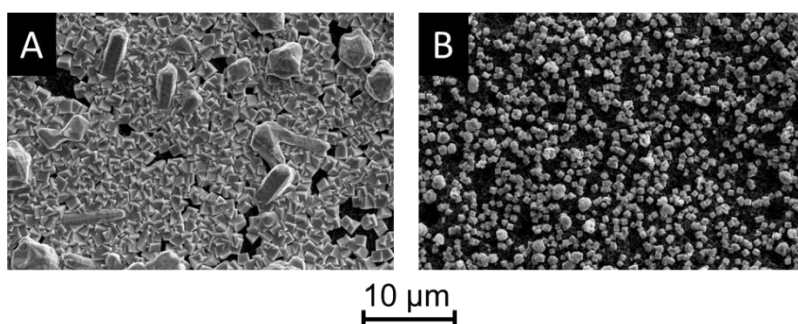


Figure S5. SEM images taken of Cu nanocube samples, deposited from precursor solutions containing 5 mM CuSO₄ and KCl in (A) pure water or (B) in 15 V/V% IPA containing aqueous solvent mixture. In all cases, the electrodeposition was performed by the potentiodynamic protocol described in the m-s, applying 500 deposition cycles.

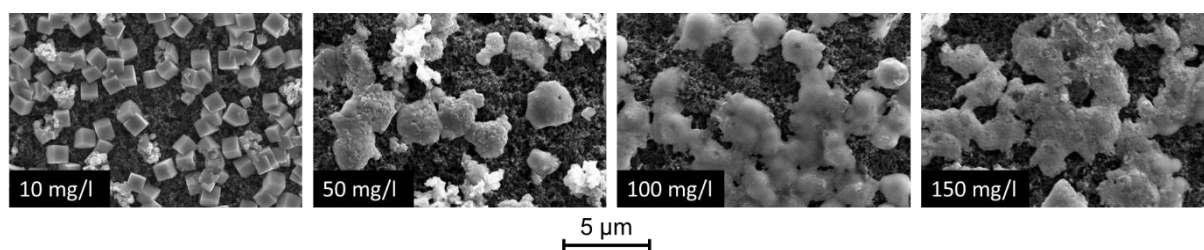


Figure S6. SEM images of Cu nanocube samples, deposited from precursor solutions containing 5 mM CuSO₄ and KCl in a 15 V/V% IPA containing aqueous solvent mixture and different amounts of Capstone ST-110 binder. In all cases, the electrodeposition was performed by the potentiodynamic protocol described in the m-s, applying 500 deposition cycles.

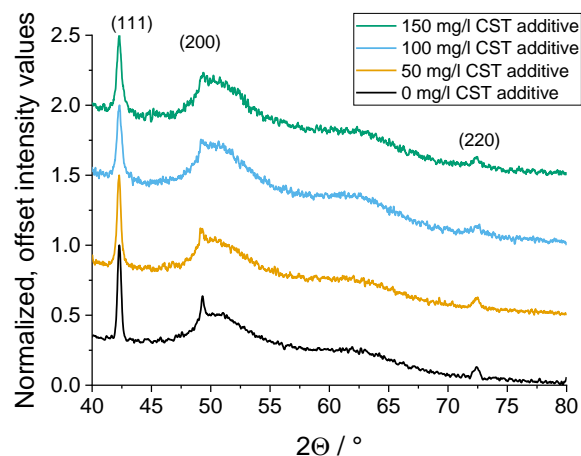


Figure S7. XRD patterns recorded for Cu nanocube samples, deposited from precursor solutions containing 5 mM CuSO_4 and KCl in a 15 V/V% IPA containing aqueous solvent mixture and different amounts of Capstone ST-110 binder. In all cases, the electrodeposition was performed by the potentiodynamic protocol described in the m-s, applying 500 deposition cycles.

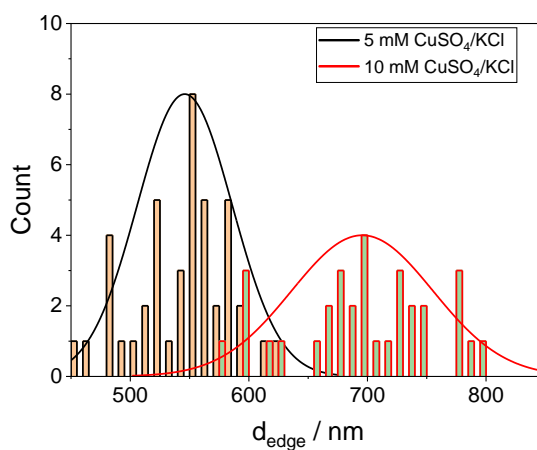


Figure S8. Size distribution of Cu nanocubes formed by electrodeposition from 5 and 10 mM CuSO_4/KCl and 15 V/V% IPA containing aqueous solutions.

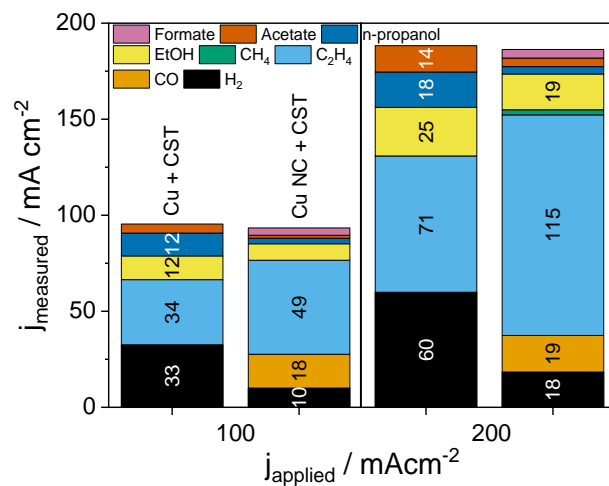


Figure S9. Product distribution during galvanostatic CO₂RR experiments on Cu nanoparticles and Cu NC catalyst layers (electrodeposited from 15 V/V% IPA and 100 mg dm⁻³ CST containing 5 mM CuSO₄/KCl solution). All measurements were performed at room temperature in a microfluidic electrolyzer cell, with a cathodic CO₂ feed of 20 cm³ min⁻¹ and with a 1 M KOH solution flowing between the electrodes at a rate of 0.5 cm³ min⁻¹. The electrodeposited GDEs were formed by 500 times repeating the potentiodynamic deposition protocol shown in Fig. 3A.

Table S1. Faradaic efficiency values calculated for all the figures presented in the m-s.

Figure 4B											
$j_{total} / \text{mA cm}^{-2}$	c(CuSO ₄ /KCl) / mM	IPA content / V/V%	c(CST) / mg/l	Faradaic efficiency / %							
				H ₂	CO	C ₂ H ₄	CH ₄	EtOH	n-PrOH	Acetate	Formate
50	5	0	0	46.4	0.0	46.3	3.3	3.2	0.0	0.3	0.3
	10	0	0	56.0	0.0	38.9	0.0	3.1	0.5	0.2	0.2
	5	15	0	20.2	28.9	41.7	0.0	2.8	0.7	0.3	1.1
	10	15	0	15.7	29.5	53.4	0.0	3.6	1.1	0.7	1.6
100	5	0	0	69.4	0.0	12.0	5.8	1.8	0.0	0.3	0.3
	10	0	0	67.7	0.0	18.7	3.4	2.4	0.3	0.3	0.3
	5	15	0	10.6	14.9	46.0	1.9	4.0	0.9	0.7	1.0
	10	15	0	10.8	16.1	52.6	0.9	4.5	1.0	0.8	0.9
200	5	0	0	71.1	0.0	0.0	0.0	0.4	0.0	0.1	0.1
	10	0	0	79.3	0.0	0.0	0.0	0.4	0.0	0.1	0.0
	5	15	0	16.2	4.0	43.6	12.9	4.1	0.5	1.8	0.8
	10	15	0	15.0	6.2	50.9	7.0	4.1	0.5	1.7	0.8

Figure 4C											
$j_{total} / \text{mA cm}^{-2}$	c(CuSO ₄ /KCl) / mM	IPA content / V/V%	c(CST) / mg/l	Faradaic efficiency / %							
				H ₂	CO	C ₂ H ₄	CH ₄	EtOH	n-PrOH	Acetate	Formate
50	5	15	10	18.4	23.2	36.6	0.5	15.5	3.0	1.3	4.3
	10	15	100	12.8	26.0	40.8	0.1	27.5	3.2	8.7	5.8
	5	15	10	14.0	34.9	35.9	0.0	17.5	4.6	5.5	5.9
	10	15	100	16.7	19.2	46.3	0.5	28.1	5.0	8.1	6.1
100	5	15	10	9.3	12.2	45.5	1.3	14.4	2.6	2.0	3.0
	10	15	100	9.7	13.4	51.8	0.6	13.6	2.8	1.5	3.9
	5	15	10	10.1	17.6	48.9	0.0	8.6	2.9	1.5	3.8
	10	15	100	10.7	9.3	57.6	0.7	11.4	3.1	1.4	2.9
200	5	15	10	11.2	4.6	45.8	7.7	12.8	1.5	4.2	1.8
	10	15	100	10.0	6.9	55.5	1.1	13.1	2.2	3.3	2.5
	5	15	10	9.2	9.5	57.4	1.3	9.3	1.9	2.2	2.2
	10	15	100	24.0	3.9	40.4	7.1	11.3	1.8	2.4	2.4

Figure 5A												
$j_{total} / \text{mA cm}^{-2}$	c(CuSO ₄ /KCl) / mM	IPA content / V/V%	c(CST) / mg/l	t / min	Faradaic efficiency / %							
					H ₂	CO	C ₂ H ₄	CH ₄	EtOH	n-PrOH	Acetate	Formate
200	5	15	0	5	69.9	1.2	2.8	8.1	12.8	0.8	2.6	1.5
	10	15	0	20	89.7	1.5	0.0	0.1	0.0	0.0	0.0	0.0

Figure 5B												
$j_{total} / \text{mA cm}^{-2}$	c(CuSO ₄ /KCl) / mM	IPA content / V/V%	c(CST) / mg/l	t / min	Faradaic efficiency / %							
					H ₂	CO	C ₂ H ₄	CH ₄	EtOH	n-PrOH	Acetate	Formate
200	5	15	100	5	9.8	12.3	59.9	0.3	12.0	1.4	2.3	1.7
	10	15	100	20	8.5	6.7	59.3	0.5	15.1	2.3	3.3	1.8
	5	15	100	39	10.9	4.1	57.5	1.2	21.2	2.7	5.0	2.2
	10	15	100	58	63.5	0.2	4.8	2.2	12.0	0.9	3.1	2.0